Journal of the Iranian Chemical Society
https://doi.org/10.1007/s13738-019-01777-1

ORIGINAL PAPER

# Horsetail plant (*Equisetum arvense*) and horsetail plant ash: application and comparison of their catalytic activities as novel and natural porous lewis acid catalysts for the one-pot green synthesis of 2-amino-4*H*-chromene derivatives under solvent-free conditions

**Nina Hosseini Mohtasham**[1] · **Mostafa Gholizadeh**[1]

Received: 20 March 2019 / Accepted: 30 August 2019


**Abstract**
This study aims to use a new medicinal porous plant having a high content of silica known as horsetail and horsetail ash for the first time as novel, efficient, and environmentally friendly natural mild catalysts. The structure of these catalysts was characterized by different techniques such as FT-IR, XRF, SEM–EDS, $N_2$ adsorption–desorption, XRD, and ICP analysis. The results obtained from the analysis revealed that both horsetail and horsetail ash could act as a solid acid catalyst. In addition, a further detailed analysis illustrated that they have a different surface area, porosity, and crystalline structure which can affect their catalytic activities. The synthesis of 2-amino-4*H*-chromene derivatives was performed via a one-pot three-component condensation of dimedone, malononitrile, and various aromatic aldehydes to compare their catalytic activities under solvent-free conditions. Due to its high porosity and high surface area, horsetail ash yields better results compared to the horsetail itself. FT-IR, mass, $^1$H-NMR, and $^{13}$C-NMR spectroscopies were used to identify the synthesized compounds in this study. An important advantage of this method is the use of these effective natural catalytic systems with characteristics such as low cost, mild reaction conditions, nontoxicity, and reusability which resulted in corresponding products in high to excellent yields and proper reaction times.

**Keywords** Horsetail plant · Ash · Heterogeneous porous catalyst · One-pot reaction · 2-Amino-4*H*-chromene

## Introduction

A brief review of relevant studies has shown that green chemistry has established a stable context providing essential design criteria for the development of efficient chemical syntheses of complex and high-added-value molecules. On the other hand, multicomponent reactions have only recently been considered as major expansions of the synthetic chemist's toolbox [1]. Academic and industrial research groups have increasingly focused on multicomponent reactions (MCRs), combining at least three simple building blocks and providing the most powerful platform to access many small organic compounds such as biologically active heterocyclic compounds in a limited number of reaction steps in one pot [2]. One of the most common MCRs producing an interesting class of oxygen heterocyclic compounds is 2-amino-4*H*-chromene derivatives synthesis, with attractive pharmacological and biological features, such as antiallergic [3], antitumor [4], antimicrobial [5], antioxidant [6], anticancer [7], and antifungal properties [8]. Due to the prominence of 2-amino-4*H*-chromene derivatives, several reagents [9–15] and various synthetic methods [16–19] have been used for the synthesis of these types of heterocyclic compounds. Although these procedures provide an improvement in the synthesis of the mentioned compounds, some of the applied methods have limitations such as harsh reaction conditions, nongreen solvents, tedious steps for

**Electronic supplementary material** The online version of this article (https://doi.org/10.1007/s13738-019-01777-1) contains supplementary material, which is available to authorized users.

✉ Mostafa Gholizadeh
m_gholizadeh@um.ac.ir

Nina Hosseini Mohtasham
ninamohtasham77@gmail.com

[1] Department of Chemistry, Faculty of Science, Ferdowsi University of Mashhad, Mashhad 9177948974, Iran

Published online: 05 September 2019

the preparation of catalyst, hazardous and expensive catalysts, strongly acidic conditions, and the use of toxic metals. Recently, chemists have been interested in the development of clean and environmentally friendly approaches to substitute hazardous catalysts with more relatively environmental benign ones. The synthesis of 2-amino-4*H*-chromene has become one of the most studied subjects to present new catalysts with the weakest acids and bases. In addition to our efforts to develop new and green chemistry methods, as well as our interest in the application of eco-friendly heterogeneous catalysis of organic reactions, this study intends to report the utilization of horsetail and horsetail ash as novel, inexpensive, and available heterogeneous natural mild solid acid catalysts for the first time to synthesize 2-amino-4*H*-chromene derivatives via a one-pot three-component condensation of dimedone, malononitrile, and various aromatic aldehydes in solvent-free conditions regarding the goals of green chemistry.

In general, horsetail can be defined as a species of *Equisetum arvense*. It is a widely distributed plant in almost all parts of the world; however, it mainly grows in temperate Northern hemisphere areas of Asia, Europe, North America, and North Africa [20] (Scheme 1). Horsetail is a source of silica or silicon and it is one of the most densely silicified plants in which silica is mostly deposited in the amorphous form [21] (Fig. 5a). For decades, horsetail has been extensively applied in medicine, and researchers have believed that some of the medicinal properties of horsetail are due to its high silica content [22]. Since it is rich in silica and silicic acids, horsetail is known as a beneficial system improving the body's resistance to infections and enhancing the elasticity and resistance of the skin and connective tissue. An additional advantage of horsetail is its interesting pharmacological activities such as pain-relieving agent [23], hepatoprotective activity [24], treatment of anemia [25], antidiuretic activity [27], antimicrobial activity [28], an herbal treatment for nail disorders, skin and hair remedy, relieving rheumatism pain, beneficial for cardiovascular problems as well as its usefulness to promote the growth and stability of the skeletal structure [26] used and studied in Europe and China since ancient times.

Besides, horsetail plant is reported to contain active components such as phenolic acids (ascorbic acid, ferulic acid, salicylic acid, malic acid, caffeic acid, gallic acid, pectic acid, and tannic acid) [29, 30], saponins [31], flavonoids [30, 32], alkaloids [26], enzymes (mainly Thiaminase) [33], styrylpyrone glucosides [34], and branched long-chain dicarboxylic acid [35]. It also contains minerals such as silicon and silicates [30], potassium, calcium, aluminum, sulfur, magnesium, manganese, zinc, chrome, and cobalt [21].

It is reported that the exposure of horsetail plant to high temperature would result in the production of the horsetail ash considered to contain better properties and interestingly including higher content of silica, higher surface area, and porosity compared to horsetail plant [20]. These facts have been investigated using some analysis which their results are further discussed.

The relevant studies in green chemistry, in which the application of a novel, eco-friendly, nontoxic, inexpensive, stable, and recyclable catalysts is considered very significant as well as the above-mentioned subjects about the unique properties of horsetail and horsetail ash (e.g., the active compounds and some metals), encouraged us to apply horsetail and horsetail ash as an abundant, green, and natural Lewis acid catalysts in organic reactions for the synthesis of 2-amino-4*H*-chromene derivatives via a mild reaction of dimedone (1), malononitrile (2), and various aromatic aldehydes (3) and consequently make a comparison between the catalytic activities of horsetail and horsetail ash (Scheme 2).


**Scheme 1** Image of horsetail plant, **a** as reported in the literature, **b** before its application in this research

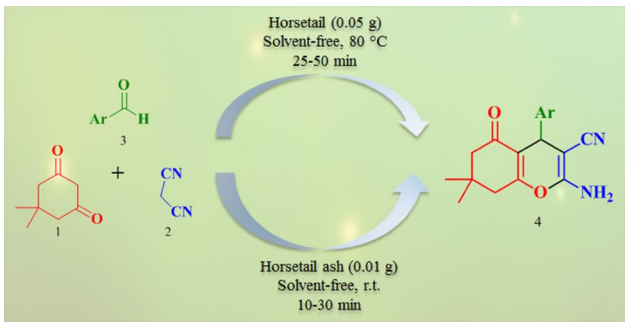


**Scheme 2** Synthesis of 2-amino-4*H*-chromene derivatives catalyzed by horsetail and horsetail ash

## Experimental section

### Materials and analytical methods

All the starting materials used for the synthesis in this study were purchased from Merck and Sigma-Aldrich companies and applied without further purification. The purity determination of the substrate and reaction monitoring was performed by TLC on silica gel polygram STL G/UV 254 plates. The melting points of products were determined by Electrothermal Type 9100 melting point apparatus. The $^{1}$H NMR and $^{13}$C NMR spectra were run on a Bruker Avance, at 300 and 75 MHz, respectively, using TMS as an internal standard and DMSO-$d_6$ as the solvent. Mass analysis was performed by Agilent Technology (HP) 5973, mass spectrometer operating at an ionization potential of 70 eV. The FT-IR spectra were recorded from KBr disk within the range of 400–4000 $cm^{-1}$ using an AVATAR 370 FT-IR Therma Nicolet spectrometer. Chemical compositions of horsetail and horsetail ash were analyzed using X-ray fluorescence spectroscopy (XRF) (model PW1410, Philips). Elemental compositions were determined with a Leo 1450 VP scanning electron microscope equipped with an SC7620 energy-dispersive spectrometer (SEM–EDS) presenting a 133 eV resolution at 20 kV. The surface area, pore volume, and average pore diameter were measured by BELSORP MINI (Quantachrome, USA). Surface areas of the samples were measured by adsorption of nitrogen gas at 77 K and the application of Brunauer–Emmett–Teller (BET) calculation, whereas pore size and pore size distribution were determined using the methods proposed by Barrett, Joyner, and Halenda (BJH) and by Dollimore and Heal (DH). The crystal phases of the catalyst were examined by X-ray diffraction (XRD) using a D8 ADVANCE Bruker diffractometer operated at 40 kV and 30 mA, using CuKα radiation ($k = 0.154$ Å), in the $2\theta$ range from 10° to 80°. Inductively coupled plasma (ICP) was studied on a SPECTRO ARCOS ICP-OES analyzer instrument (model 76004555).

All yields refer to isolated products. Furthermore, the known products were identified through comparing their spectral and physical data with those of the previously reported data or with the authentic samples.

### Preparation of horsetail and horsetail ash as catalysts

Horsetail plant was purchased from the market, Mashhad, Iran, washed several times with distilled water to remove any adhering and cleaving materials, and dried at room temperature for 24 h. Then the dried plant was smashed and sieved (80-mesh size), again washed with distilled water, and dried at 110 °C for 5 h. After thermal processing of the horsetail at 400 °C for 12 h, the horsetail ash was obtained (Scheme 3). The removal of the organic matrix (e.g., cellulose, hemicellulose, pectin) by calcination at 400 °C resulted in an open porosity with a high surface area of about 162 $m^2/g$ for horsetail ash compared to horsetail (Table 3). However, as the calcination temperature increased, the surface area decreased continuously to a value close to zero at 750 °C [20]. Therefore, the optimum calcination temperature appears to be around 400 °C.

### General procedure for the synthesis of 2-amino-4*H*-chromene derivatives (4a–r) using horsetail and horsetail ash as catalysts

In a typical procedure, a mixture of dimedone (1 mmol), aromatic aldehydes (1 mmol), and malononitrile (1.5 mmol) was stirred thoroughly in the presence of a catalytic amount of powdered horsetail (0.05 g) at 80 °C in solvent-free conditions for an appropriate period of time as mentioned in Table 7. After the reaction was completed (monitored by TLC: *n*-hexane/ethyl acetate 4:1 as eluent), hot ethanol (5 ml) was added, and the catalyst (horsetail) was separated by filtration, washed two times with ethanol, and dried in vacuum oven to be reused in subsequent reactions. The filtrate was concentrated in vacuum, and upon cooling, a solid product was obtained. The pure products were obtained in their crystalline forms by recrystallization from ethanol, and

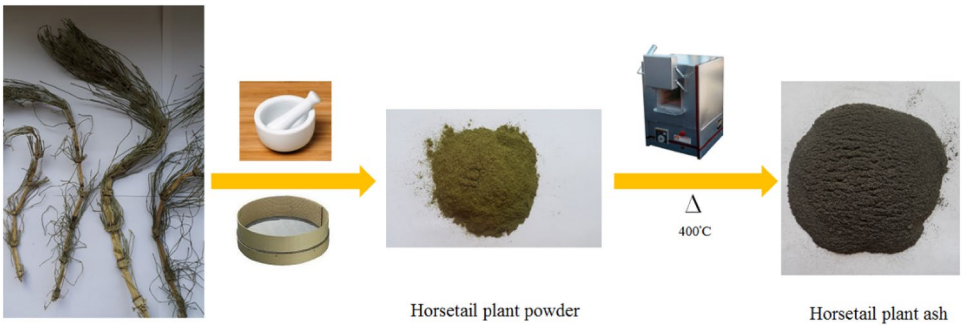


**Scheme 3** Preparation of horsetail and horsetail ash

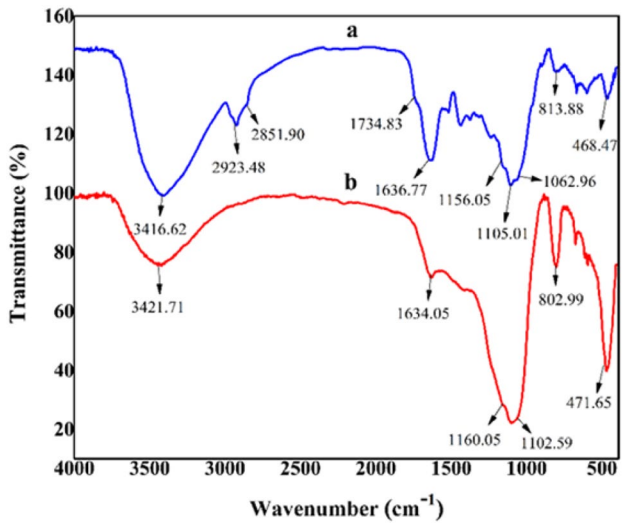


**Fig. 1** FT-IR spectrum of **a** horsetail and **b** horsetail ash

no more purification was required. All the products were known compounds which were identified by the characterization of their melting points (as indicated in Table 7) in comparison with those authentic literature samples and also in some cases by their FT-IR, mass, $^{1}$H NMR, and $^{13}$C NMR spectral data. Also, owing to the catalytic properties of horsetail ash, it was decided to carry out the reaction again in the presence of horsetail ash as the catalyst. Afterward, the results obtained from horsetail and horsetail ash as two different catalytic systems were compared to understand which of them could act as a better catalytic system for catalyzing this reaction. The obtained results revealed that in comparison with horsetail, only a small amount of horsetail ash was needed as a catalyst (0.01 g), and the reaction could also be carried out at room temperature. These results could be due to the high surface area and high porosity of horsetail ash considered as its main characteristics rather than the horsetail plant that provides a good reaction condition. The results were compared with each other and then are summarized in Table 7.

## Results and discussion

### Characterization of catalysts

#### FT-IR analysis of the catalysts

Figure 1 shows the FT-IR spectra of horsetail and horsetail ash. As illustrated in Fig. 1a, the broadband at around 3500–3400 $cm^{-1}$ is assigned to the stretching vibration of Si–O–H band and the H–O–H vibration of water molecule adsorbed on the silica surface [36]. The doublet bands at about 2923 and 2851 $cm^{-1}$ are related to the C–H stretching from aliphatic saturated compounds [37]. A weak peak around 1734 $cm^{-1}$ was proposed to be attributed to the C=O stretching of the related organic compounds [38]. Furthermore, the band detected at about 1640–1620 $cm^{-1}$ comes from the bending vibration of water molecules. The strong peaks between 1100 and 1025 $cm^{-1}$ are due to the asymmetric stretching vibration of the structural siloxane band, Si–O–Si. The bands at 805–800 and 475–460 $cm^{-1}$ in all spectra are assigned to the Si–O–Si symmetric stretching vibration and Si–O–Si bending vibration, respectively [39]. As shown in Fig. 1b, the exposure of horsetail plant to high temperature resulted in the removal of all organic group peaks forming the horsetail ash.

#### XRF analysis of the catalysts

XRF technology provides one of the simplest and most accurate procedures for the determination of chemical compositions of many types of materials.

The chemical composition of horsetail ash that was determined by XRF showed a high value of silica content for the sample (up to 85%). Horsetail ash also includes other compositions such as $Al_2O_3$, $Fe_2O_3$, $SO_3$, $P_2O_5$, $K_2O$, $Na_2O$, and CaO as a very small proportion of metallic elements (Table 1). Also, the main components of horsetail were also determined and are listed in Table 2. As it is shown in Table 2, the amount of silica is higher than other elements. According to the results presented in Tables 1 and 2, it can

**Table 1** Chemical composition of horsetail ash obtained from X-ray fluorescence analysis (wt%)

| $SiO_2$ | $Al_2O_3$ | $Na_2O$ | MgO | $K_2O$ | $TiO_2$ | MnO | CaO | $P_2O_5$ | $Fe_2O_3$ | $SO_3$ |
|---|---|---|---|---|---|---|---|---|---|---|
| 85.39 | 0.07 | 0.09 | 4.32 | 0.43 | 0.03 | 0.04 | 6.24 | 0.90 | 0.75 | 1.62 |

**Table 2** Chemical composition of horsetail obtained from X-ray fluorescence analysis (wt%)

| $SiO_2$ | $Al_2O_3$ | $Na_2O$ | MgO | $K_2O$ | $TiO_2$ | MnO | CaO | $P_2O_5$ | $Fe_2O_3$ | $SO_3$ | Cl | LOI[a] |
|---|---|---|---|---|---|---|---|---|---|---|---|---|
| 15 | 0.04 | 0.12 | 0.82 | 5.89 | 0.01 | 0.02 | 4.92 | 0.42 | 0.51 | 4 | 0.85 | 68 |

[a]Loss on ignition

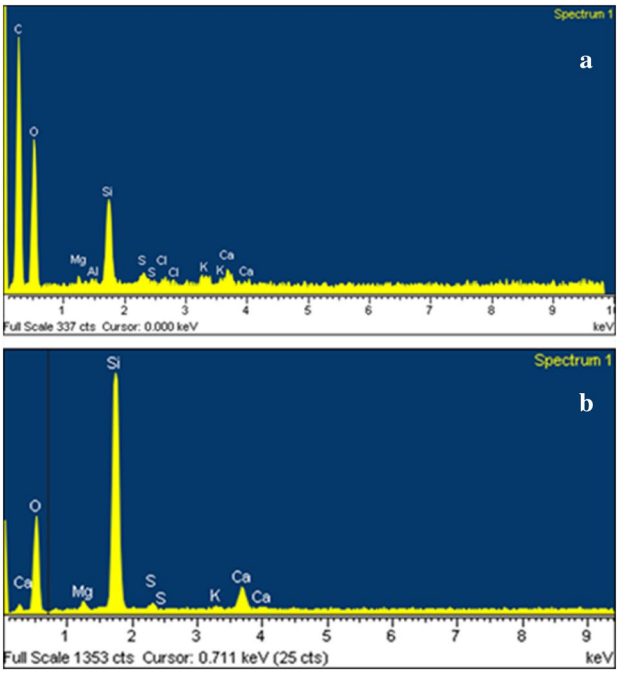


**Fig. 2** EDS spectrum of **a** horsetail and **b** horsetail ash

be concluded that the amount of silica in horsetail ash is higher than that of horsetail. The result also illustrated that the presence of such elements in both horsetail and horsetail ash results in their function as Lewis acid catalytic system.

### EDS analysis of the catalysts

The energy-dispersive spectrum (EDS) of horsetail (Fig. 2a) indicated that it included significantly high concentrations of carbon related to its organic compounds (e.g., cellulose, hemicellulose, pectin) and alkali and alkaline earth metals, for instance, Si, Ca, K, Mg, S, Al, as the main components [40]; however, the concentration of silica was revealed to be higher than that of other metals. In EDS analysis of horsetail ash (Fig. 2b), achieved at a high temperature (400 °C), the peak related to organic parts has not been observed, indicating that all organic compounds have been removed. Also, a high concentration of Si was detected which is consistent with the XRF results.

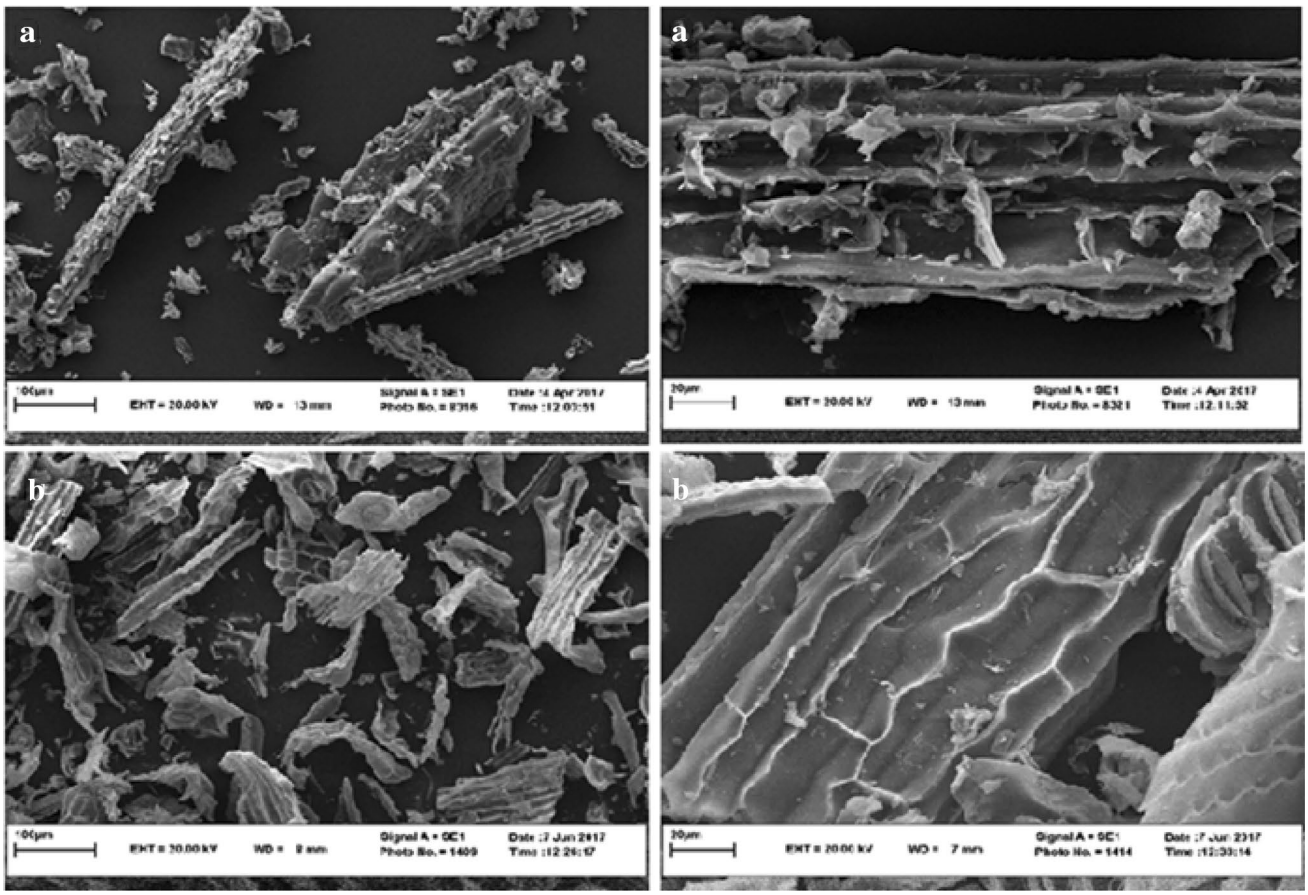


**Fig. 3** SEM images of **a** horsetail and **b** horsetail ash

### SEM analysis of the catalysts

In further analyses of this research, the scanning electron microscope (SEM) was considered as a useful tool to analyze the surface morphology of the horsetail compared to horsetail ash (Fig. 3).

As illustrated, silicon was found at its highest amount in the outer edge of both horsetail and horsetail ash [40]. Moreover, it seemed as if the horsetail ash (Fig. 3b) perfectly retained the original structure of the horsetail plant (Fig. 3a). Also, as indicated in Fig. 3b, it can be estimated that the removal of organic compounds resulted in the development of a higher surface area and porosity for horsetail ash in which it could provide a larger contact area for catalyzing the reaction in better conditions rather than that of horsetail.

### N2 adsorption–desorption studies

The nitrogen adsorption–desorption isotherms and pore size distribution curves of horsetail and its ash are shown in Fig. 4a–d. As indicated in Fig. 4a, horsetail showed

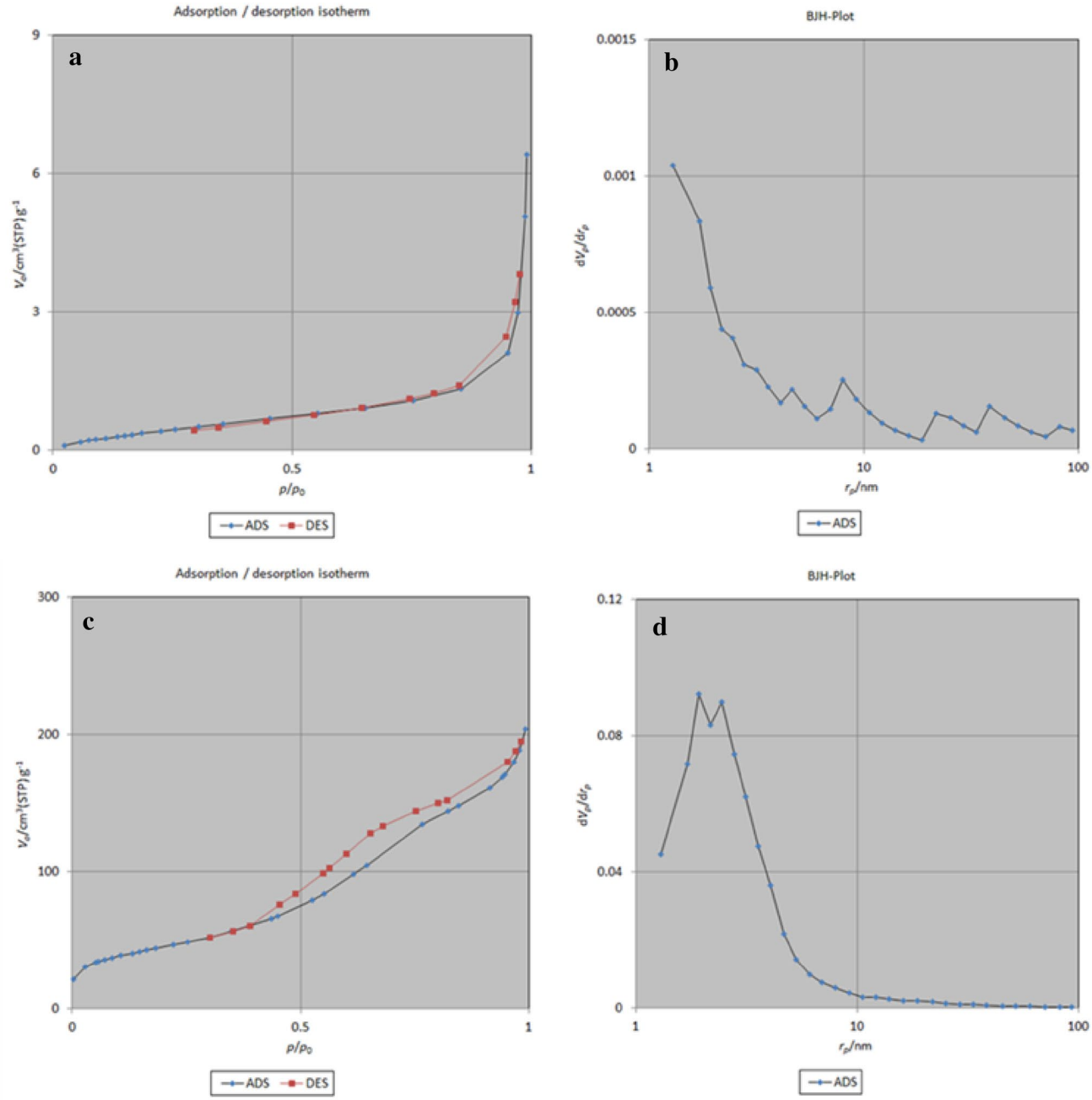


**Fig. 4** N2 adsorption–desorption isotherms and pore size distributions of horsetail plant (**a**, **b**) and horsetail ash (**c**, **d**)

**Table 3** Specific surface area ($S_{BET}$), pore volume, and mean pore diameter of horsetail and horsetail ash

| Sample | $S_{BET}$ ($m^2\ g^{-1}$) | Pore volume ($cm^3\ g^{-1}$) | Mean pore diameter (nm) |
|---|---|---|---|
| Horsetail | 2.025 | 0.0094 | 7.633 |
| Horsetail ash | 162.98 | 0.311 | 18.574 |

the characteristics of type II isotherm with H3-type hysteresis loops which confirm the existence of porous structure (mesoporous or macroporous structure) according to the classification presented by IUPAC [41]. Furthermore, the pore size distribution curves (based on the Barrett–Joyner–Halenda (BJH) method) displayed that the pore size distribution is rather broad compared to that of its ash having considerable irregular pore size distribution (Fig. 4b). Also, as shown in Fig. 4c, a typical type IV isotherm with an H1 hysteresis loop was present for horsetail ash, indicating the characteristic of mesoporous silica network [42]. Also, the BJH pore size calculations demonstrated a uniform pore size distribution with a high-intensity peak, which proves the high regularity of the mesostructure (Fig. 4d). The specific surface area, pore volume, and mean pore diameter for both horsetail and horsetail ash are shown in Table 3. A close examination of the data listed in Table 3 determined the higher surface area of the horsetail ash compared to the horsetail due to its exposure to high temperature, resulting in the successful removal of all organic compounds. Also, it is shown that pore volume and mean pore diameter of horsetail ash both increased after burning the horsetail plant [20]. Therefore, all obtained data determined that the presence of horsetail ash in the reaction resulted in the formation of better reaction conditions due to its high surface area and porosity, confirming the SEM analyses results.

### X-ray diffraction (XRD) analysis of the catalysts

The XRD patterns of the horsetail and horsetail ash are shown in Fig. 5. In horsetail pattern (Fig. 5a), a broad peak appeared around $2\theta$ equal to 22°, indicating that the silica of the horsetail was mainly in the form of amorphous [43]. This area is also overlapped by broad reflections from cellulose compounds. As observed in Fig. 5b, when horsetail was exposed to heat intervention, the broad region attributed to amorphous silica in Fig. 5a disappeared, and some minor and new sharp reflections form of the silica started to appear revealing the fact that most amorphous silica has been transformed into α-quartz ($SiO_2$). Also, no cellulose reflections

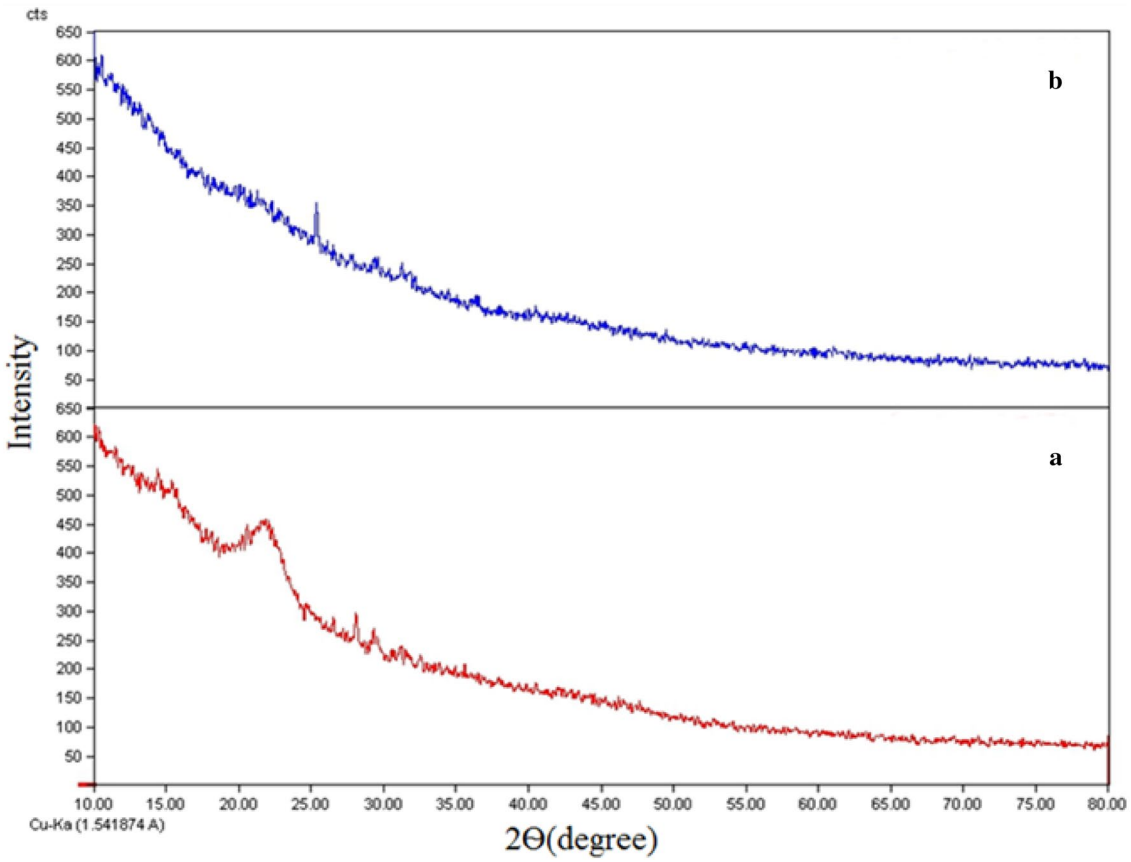


**Fig. 5** XRD patterns of **a** horsetail and **b** horsetail ash

**Table 4** Elemental analysis for both horsetail and horsetail ash

| Element | Elemental content of horsetail plant (ppm) | Elemental content of horsetail plant ash (ppm) |
|---|---|---|
| Ca | 40,121.5 | 39,551.0 |
| Al | 28,979.8 | 23,672.7 |
| K | 26,814.1 | 9936.2 |
| Mg | 18,375.3 | 28,767.1 |
| Na | 1098.65 | 8295.2 |
| P | 9771.83 | 13,273.3 |
| Ba | 9659.63 | 8585.5 |
| S | 2962.2 | 2433.6 |
| Fe | 1487.6 | 2640.2 |
| Zn | 767.271 | 701.8 |
| Cu | 111.149 | 68.4 |
| Sr | 279.427 | 487.5 |
| Sb | 19.239 | 27.6 |
| Mn | 280.3 | 288.1 |
| Si | 60,979.1 | 303,456.6 |

**Table 5** Optimization of the amount of catalyst, solvent, and temperature in a one-pot synthesis of the model reaction

| Entry | Amount of catalyst (g) | Solvent | Temperature | Time (min) | Yield[a] (%) |
|---|---|---|---|---|---|
| 1 | – | – | r.t. | 70 | 30 |
| 2 | – | – | 110 °C | 70 | 45 |
| 3 | 0.01 | – | r.t. | 10 | 99 |
| 4 | 0.01 | – | 60 °C | 10 | 99 |
| 5 | 0.01 | – | 110 °C | 10 | 99 |
| 6 | 0.03 | – | r.t. | 10 | 98 |
| 7 | 0.005 | – | r.t. | 25 | 80 |
| 8 | 0.01 | $H_2O$ | Reflux | 20 | 80 |
| 9 | 0.01 | EtOH | Reflux | 15 | 90 |
| 10 | 0.01 | $CH_2Cl_2$ | Reflux | 30 | 83 |

Reaction condition: 4-nitrobenzaldehyde (1 mmol), malononitrile (1.5 mmol), dimedone (1 mmol) when horsetail ash was used as a catalyst

[a]Isolated yield

were detected in horsetail ash pattern, illustrating that all organic substances were successfully removed after heating.

These results confirmed the ones obtained from FT-IR, EDS, and XRF analyses.

### Elemental analysis of the catalysts

The elemental contents of both horsetail and horsetail ash (0.1 g) were determined and characterized using inductively coupled plasma (ICP) technique presenting the following output (Table 4).

**Table 6** Optimization of the amount of catalyst, solvent, and temperature in a one-pot synthesis of the model reaction

| Entry | Amount of catalyst (g) | Solvent | Temperature | Time (min) | Yield[a] (%) |
|---|---|---|---|---|---|
| 1 | – | – | r.t. | 70 | 30 |
| 2 | – | – | 110 °C | 70 | 45 |
| 3 | 0.01 | – | r.t. | 70 | 60 |
| 4 | 0.01 | – | 110 °C | 60 | 70 |
| 5 | 0.03 | – | 110 °C | 45 | 78 |
| 6 | 0.05 | – | 110 °C | 25 | 90 |
| 7 | 0.05 | – | 80 °C | 25 | 90 |
| 8 | 0.05 | – | 60 °C | 35 | 85 |
| 9 | 0.07 | – | 80 °C | 25 | 90 |
| 10 | 0.05 | $H_2O$ | Reflux | 30 | 85 |
| 11 | 0.05 | EtOH | Reflux | 30 | 87 |
| 12 | 0.05 | $CH_2Cl_2$ | Reflux | 35 | 85 |

Reaction condition: 4-nitrobenzaldehyde (1 mmol), malononitrile (1.5 mmol), dimedone (1 mmol) when horsetail was used as a catalyst

[a]Isolated yield

The obtained results confirmed the presence of some elements in both horsetail and horsetail ash, creating an acidic property for both of them. The results also confirm that the amount of silica in horsetail ash is higher than that of horsetail. These results are in good agreement with those obtained from XRF and EDS analyses.

## Catalytic test

Based on the data obtained from the present study on horsetail and horsetail ash, and according to their unique properties, we estimated that they might be used as efficient green natural herbal heterogeneous mild solid acid catalysts. To follow our interest and evaluate their catalytic performances, we intended to employ them for the first time as natural mild solid acid catalysts to catalyze a mild and simple reaction for the synthesis of 2-amino-4*H*-chromene derivatives (Scheme 2).

To this end, we aimed to identify the best reaction conditions for the synthesis of these compounds. Following this, 4-nitrobenzaldehyde (1 mmol), malononitrile (1.5 mmol), and dimedone (1 mmol) were chosen as a model reaction, and parameters such as the effect of catalysts, type of solvent system as well as temperature were systematically examined. Initially, different amounts of catalysts at the range of 25–110 °C under solvent-free conditions were investigated. The obtained results showed that in the absence of catalysts, only a trace amount of products was detected (Entries 1 and 2, Tables 5 and 6).

Also, as can be seen, the optimum amounts of the horsetail and horsetail ash for completing the reaction were 0.05 and 0.01 g, respectively. Notably, lower

amounts of catalysts resulted in lower yields (Entry 7, Table 5 and Entries 4 and 5, Table 6); however, higher amounts did not affect the reaction times and yields (Entry 6, Table 5 and Entry 9, Table 6). Concerning the solvent system, to compare the results of the solution with that of solvent-free conditions, the model reaction was examined using 0.01 g of horsetail ash and 0.05 g of horsetail with $H_2O$, EtOH, and $CH_2Cl_2$ under reflux conditions. As shown in Tables 5 and 6, the best results were achieved under solvent-free conditions. Consequently, as indicated in Tables 5 and 6, the best results were obtained through the use of 0.01 g horsetail ash at room temperature (Entry 3, Table 5) and 0.05 g of horsetail at 80 °C (Entry 7, Table 6) under solvent-free conditions.

After identifying the optimized reaction conditions, we aimed to study the application of these catalysts and compare their activity, efficiency, and scope by extending our study under these optimized conditions using horsetail (0.05 g at 80 °C) and horsetail ash (0.01 g at room temperature) with various aromatic aldehydes, dimedone, and malononitrile to give a series of 2-amino-4*H*-chromene derivatives under solvent-free conditions (Table 7). As shown in Table 7, various aromatic aldehydes containing both electron-withdrawing and electron-releasing substituents on their aromatic rings were utilized well in this reaction and successfully converted to a wide range of substituted 2-amino-4*H*-chromenes with good to excellent yields. The data in Table 7 indicate that horsetail ash is not only very effective in minimizing the reaction time, but also highly efficient in terms of catalyst amount and product yields. These advantages can be attributed to its high level of activity due to its high porosity and high surface area. The formation and purity of the products were confirmed by their melting points determination, which were in good accordance with the literature values. Moreover, the structures of some of the products were well

**Table 7** Synthesis of 2-amino-4*H*-chromene derivatives catalyzed by horsetail and horsetail ash

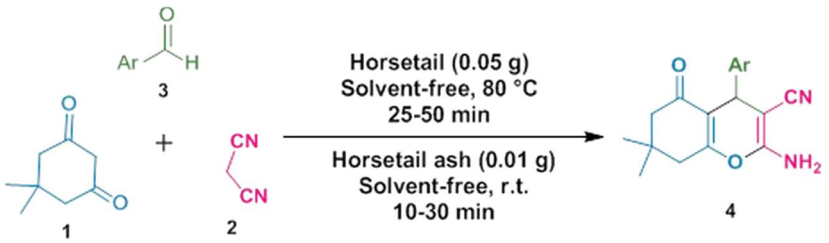


| Entry | Ar | Product | Horsetail | Horsetail ash | Melting point (°C) | |
|---|---|---|---|---|---|---|
| | | | Time[a]/yield[b] | Time[a]/yield[b] | Found | Reported (ref.) |
| 1 | $C_6H_5$ | 4a | 30/83 | 15/95 | 227–228 | 232–234 [44] |
| 2 | 4-Cl-$C_6H_4$ | 4b | 35/85 | 10/98 | 205–207 | 206–208 [45] |
| 3 | 4-$NO_2$-$C_6H_4$ | 4c | 25/90 | 10/99 | 174–175 | 178–179 [46] |
| 4 | 3-$NO_2$-$C_6H_4$ | 4d | 30/89 | 15/97 | 210–212 | 209–211 [47] |
| 5 | 4-Br-$C_6H_4$ | 4e | 25/91 | 10/98 | 206–208 | 207–209 [48] |
| 6 | 3-Br-$C_6H_4$ | 4f | 25/89 | 12/97 | 226–228 | 229–230 [49] |
| 7 | 4-Me-$C_6H_4$ | 4 g | 35/86 | 15/95 | 214–215 | 216–218 [50] |
| 8 | 3-Me-$C_6H_4$ | 4 h | 30/88 | 15/93 | 220–222 | 224–225 [49] |
| 9 | 4-OH-$C_6H_4$ | 4i | 30/85 | 10/96 | 207–209 | 210–212 [50] |
| 10 | 3-OH-$C_6H_4$ | 4j | 35/87 | 20/95 | 229–231 | 226–228 [45] |
| 11 | 2-OH-$C_6H_4$ | 4k | 30/85 | 15/94 | 244–245 | 247–249 [50] |
| 12 | 4-MeO-$C_6H_4$ | 4l | 30/90 | 15/96 | 199–201 | 201–202 [51] |
| 13 | 4-$Me_2N$-$C_6H_4$ | 4m | 35/80 | 25/93 | 214–215 | 213–215 [52] |
| 14 | 3, 4-di-OH-$C_6H_3$ | 4n | 25/91 | 15/100 | 240–241 | 241–243 [45] |
| 15 | 2-Furyl | 4o | 50/83 | 30/91 | 222–224 | 226–228 [52] |
| 16 | 2-Thienyl | 4p | 45/85 | 20/93 | 215–217 | 216–218 [53] |
| 17 | 1-Naphthyl | 4q | 40/86 | 25/95 | 214–216 | 216–218 [54] |
| 18 | 5-Br-2OH-$C_6H_3$ | 4r | 35/91 | 25/94 | 192–194 | 190–193 [55] |

[a]The reaction completion time

[b]The yields refer to pure isolated products

**Table 8** Comparison of results obtained in this research with some of those reported in the literature for the synthesis of compound 4c

| Entry | Catalyst | Reaction condition | Time (min) | Yield[a] (%) | References |
|---|---|---|---|---|---|
| 1 | $PhB(OH)_2$ (5 mol%) | $EtOH/H_2O$, reflux | 30 | 88 | [56] |
| 2 | $SiO_2$ NPs (5 mg) | EtOH, r.t. | 30 | 97 | [57] |
| 3 | Piperazine (15 mol%) | Ball milling at r.t. | 27 | 92 | [51] |
| 4 | TMU-17-$NH_2$ [b] (6 mol%) | EtOH, reflux | 240 | 96 | [58] |
| 5 | SILC[c] (0.05 g) | 80 °C | 15 | 95 | [53] |
| 6 | 20Ca-Zr-$O_2$ (50 mg) | Water + ethanol (1:1,3 ml) | 60 | 90.2 | [59] |
| 7 | OPSF (5 mg) | EtOH, r.t. | 12 | 93 | [60] |
| 8 | MSNs[d] (10 mg) | EtOH/60 °C | 10 | 95 | [61] |
| 9 | $[DiEG(mim)_2][OH]_2^e$ (10 mol%) | $H_2O$, r.t., $K_2CO_3$ | 15 | 90 | [62] |
| 10 | SB-DABCO [f] (0.06 g) | EtOH, r.t. | 20 | 90 | [63] |
| 11 | $SO4^{2-}$@MCM-41 (25 mg) | EtOH, reflux | 30 | 85 | [64] |
| 12 | $I_2$ (10 mmol%) | DMSO, 120 °C | 240 | 85 | [65] |
| 13 | $NH_4H_2PO_4$–$Al_2O_3$ (0.03 g) | Solvent free | 30 | 92 | [66] |
| 14 | TSA[g] (10 mg) | EtOH, reflux | 10 | 94 | [67] |
| 15 | $K_2CO_3$ (20 mol%) | Grinding, r.t. | 16 | 87 | [68] |
| 16 | $NH_4Al(SO_4)_2.12H_2O$ (0.2 g) | EtOH, reflux | 130 | 93 | [69] |
| 17 | Pure $SiO_2$ (0.05 g) | Solvent free, 80 °C | 35 | 75 | – |
| 18 | Pure $SiO_2$ (0.01 g) | Solvent free, r.t. | 55 | 65 | – |
| 19 | Horsetail (0.05 g) | Solvent free, 80 °C | 25 | 90 | This work |
| 20 | Horsetail ash (0.01 g) | Solvent free, r.t. | 10 | 99 | This work |

Reaction condition: 4-nitrobenzaldehyde, malononitrile, and dimedone

[a]Isolated yield, [b](Zn($NH_2$-BDC)(4-bpdb))-2DMF (TMU-17-$NH_2$, TMU corresponds to Tarbiat Modares University), [c]supported ionic liquid catalyst, [d]well-ordered mesoporous silica nanoparticles, [e]diethylene glycol-bis(3-methylimidazolium) dihydroxide, [f]silica-bonded *n*-propyl-4-aza-1-azoniabicyclo[2.2.2]octane chloride, [g]nano-titania sulfuric acid

characterized using FT-IR, mass, $^1$H NMR, and $^{13}$C NMR spectral data.

Finally, a comparison was made between the protocol reported in previous studies and that of the current study for the synthesis of 4c, as a model compound. The results summarized in Table 8 revealed that the protocol introduced in this research, which uses horsetail ash, could also be the best protocol of choice for the synthesis of these compounds. Besides, we decided to use pure silica under the exact condition in which horsetail and horsetail ash were applied, and the results are given in Table 8 (Entries 17 and 18). Interestingly, the consequence of using pure silica as catalyst was not satisfying, indicating that horsetail and horsetail ash are good acidic catalysts since not only they contain silica, but also they contain some metallic elements (e.g., Ca, K, Mg, etc.) making them better acidic catalysts compared to the pure silica, itself.

## Proposed the probable mechanism

The suggested mechanism for the synthesis of 2-amino-4*H*-chromene derivatives which is shown in Scheme 4 includes three major steps: Knoevenagel condensation, Michael addition, and finally intramolecular ring closure [70]. First, we assumed that a Knoevenagel condensation between malononitrile (2) with the carbonyl group of aldehyde (3) which is activated via the solid acid catalysts led to the formation of intermediate (5) followed by a dehydration step (6). After that, dimedone (1) was converted to its enol form after tautomerization and attacked the electrophilic center of (6) as Michael acceptor to form intermediate (7). Finally, tautomerism and intramolecular cyclocondensation of (7) produced (8), which was converted to the desired product (4). Herein, all metallic ions existing in both horsetail and horsetail ash are responsible for catalyzing the reaction effectively, but in the case of horsetail ash due to its specific structural and textural properties, it could provide larger interfacial surface area for reaction and thus enhance its activity.

## Recyclability of the catalysts

As the properties of an efficient heterogeneous catalyst, its reusability is a principal advantage to be considered that is very important for commercial and industrial applications. Hence, this study intended to investigate the reusability of these catalytic systems (horsetail and horsetail ash). For this purpose, as mentioned before, dimedone (1 mmol), 4-nitrobenzaldehyde (1 mmol), and malononitrile (1.5 mmol) were used as a model reaction. When the

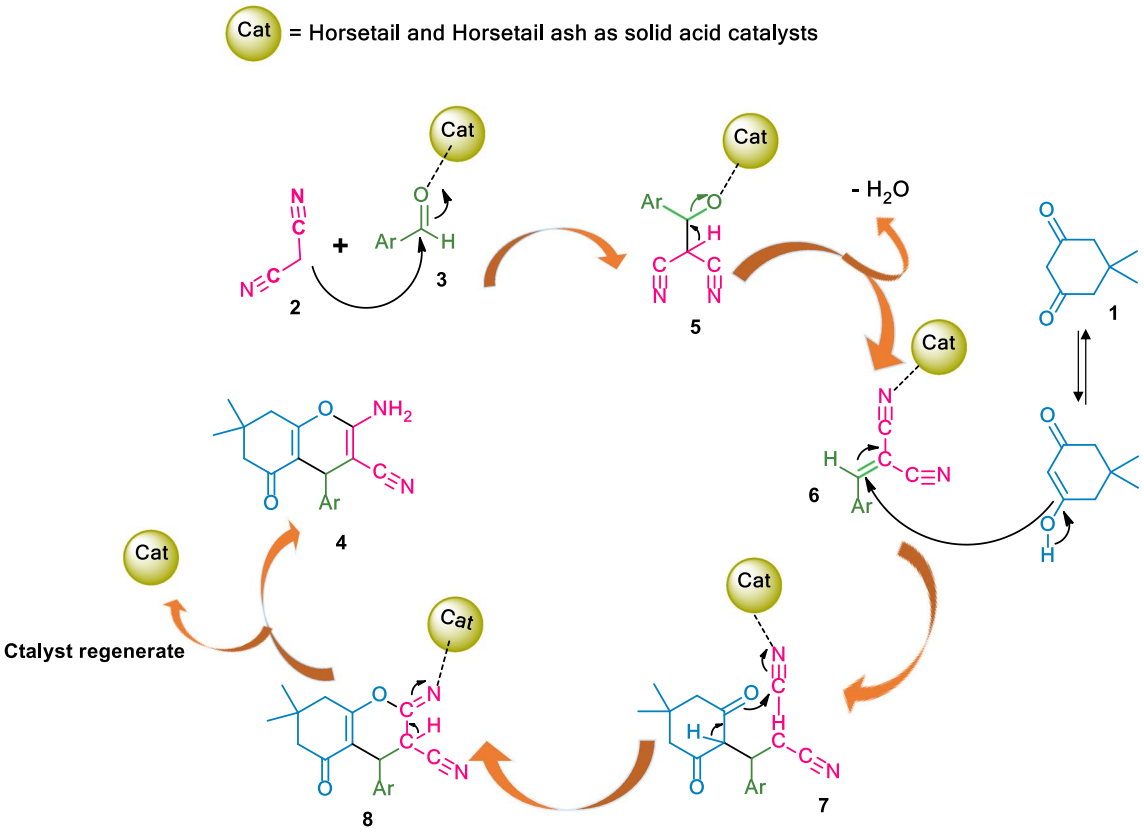


**Scheme 4** Proposed mechanism for the synthesis of 2-amino-4*H*-chromene derivatives in the presence of horsetail and horsetail ash as catalysts

reaction finished, the mixture was diluted with hot EtOH, and the catalysts were easily separated from the product by simple filtration. These remaining catalysts were further washed with ethanol to remove the residual products and were dried at 50 °C overnight. Then, the reused catalysts were exploited in another reaction indicating that horsetail and horsetail ash were reusable catalysts; however, a slight decrease in the yields of the products was observed after five cycles (Fig. 6).


**Fig. 6** Catalytic activity of reused horsetail ash versus horsetail in five cycles for the synthesis of compound 4c

## Conclusion

The present study offered an introduction of horsetail plant with its unique properties. The aim of the study was to raise awareness about this cheap, natural, and herbal green plant. According to the results of the current study, the exposure of horsetail to a high temperature resulted in the production of the horsetail ash containing better properties and advantages rather than the horsetail, itself. Furthermore, different analytical techniques were employed to identify properties and chemical compositions of each of which, specifically. The results have shown that both horsetail and horsetail ash could act as good solid acid catalytic systems. Therefore, to make a comparison between their catalytic properties, both of them were employed for the first time in the organic reaction to synthesize the 2-amino-4*H*-chromene derivatives. Consequently, it was found that in the presence of horsetail ash, the reaction took place in better conditions due to its high surface area and high porosity, providing a large contact area for catalyzing the reaction. The promising points of this

work are referred to as simple experimental procedures, total removal of problems associated with organic solvents, and the use of green, inexpensive, and nontoxic natural material as catalysts, along with its ease of preparation presenting it as a useful and attractive strategy in view of economic and environmental advantages. It is recommended that the horsetail ash could be used as a support for the preparation of various types of catalysts due to its high surface area and high silica content that could act as a natural silica resource having mesoporous structure. As a result, studies on practical applications of horsetail ash as good support for further modifications and production of various types of catalysts and their applications in other organic reactions are currently in progress in our laboratory.

**Acknowledgements** We are thankful to Ferdowsi University of Mashhad Research Council for financial support to this work (Grant No: 3/45801).

## Compliance with ethical standards

**Conflict of interest** The authors declare that they have no conflict of interest.

## References


1. R.C. Cioc, E. Ruijter, R.V.A. Orru, Green Chem. **16**, 2958 (2014)
2. T.J.J. MŘller, R.V.A. Orru, V.A. Chebanov, Y.I. Sakhno, V.E. Saraev, E.A. Muravyova, A.Y. Andrushchenko, S.M. Desenko, V.R. Akhmetova, G.R. Khabibullina, *Multi-component Reactions In Heterocyclic Chemistry* (Springer, New York, 2011), pp. 31–73
3. K. Görlitzer, A. Dehne, E. Engler, Arch. Pharm. **316**, 264 (1983)
4. S.J. Mohr, M.A. Chirigos, F.S. Fuhrman, J.W. Pryor, Cancer Res. **35**, 3750 (1975)
5. T. Raj, R.K. Bhatia, R.K. Sharma, V. Gupta, D. Sharma, M.P.S. Ishar, Eur. J. Med. Chem. **44**, 3209 (2009)
6. P. Vats, V. Hadjimitova, K. Yoncheva, A. Kathuria, A. Sharma, K. Chand, A.J. Duraisamy, A.K. Sharma, A.K. Sharma, L. Saso, S.K. Sharma, Med. Chem. Res. **23**, 4907 (2014)
7. M.K. Manion, D. Hockenbery, Cancer Biol. Ther. **2**, 104 (2003)
8. Z.Q. Xu, K. Pupek, W.J. Suling, L. Enache, M.T. Flavin, Bioorg. Med. Chem. **14**, 4610 (2006)
9. E. Mosaddegh, A. Hassankhani, G. Mansouri, E.-J. Chem. **8**, 529 (2011)
10. A. Khazaei, F. Gholami, V. Khakyzadeh, A.R. Moosavi-Zare, J. Afsar, RSC Adv. **5**, 14305 (2015)
11. Y. Ren, W. Zhang, J. Lu, K. Gao, X. Liao, X. Chen, RSC Adv. **5**, 79405 (2015)
12. H.R. Safaei, M. Shekouhy, S. Rahmanpur, A. Shirinfeshan, Green Chem. **14**, 1696 (2012)
13. M.R. Islami, E. Mosaddegh, Phosphorus Sulfur **184**, 3134 (2009)
14. X.-S. Wang, D.-Q. Shi, S.-J. Tu, C.-S. Yao, Synth. Commun. **33**, 119 (2003)
15. S. Balalaie, M. Sheikh-Ahmadi, M. Bararjanian, Catal. Commun. **8**, 1724 (2007)
16. S.-J. Tu, Y. Gao, C. Guo, D. Shi, Z. Lu, Synth. Commun. **32**, 2137 (2002)
17. I. Devi, P.J. Bhuyan, Tetrahedron Lett. **45**, 8625 (2004)
18. S. Tu, H. Jiang, Q. Zhuang, C. Miao, D. Shi, X. Wang, Y. Gao, Chin. J. Org. Chem. **23**, 488 (2003)
19. O.H. Qareaghaj, S. Mashkouri, M.R. Naimi-Jamal, G. Kaupp, RSC Adv. **4**, 48191 (2014)
20. L. Sapei, Characterisation of silica in *Equisetum hyemale* and its transformation into biomorphous ceramics, pp. 1–158 (2007)
21. G. Holzhüter, K. Narayanan, T. Gerber, Anal. Bioanal. Chem. **376**, 512 (2003)
22. D. Cloutier, A.K. Watson, Weed Sci. **33**, 358 (1985)
23. F.H.M. Do Monte, J.G. dos Santos, M. Russi, V.M.N.B. Lanziotti, L.K.A.M. Leal, G.M. de Andrade Cunha, Pharmacol. Res. **49**, 239 (2004)
24. H. Oh, D.H. Kim, J.H. Cho, Y.C. Kim, J. Ethnopharmacol. **95**, 421 (2004)
25. H. Mekhfi, M. El Haouari, A. Legssyer, M. Bnouham, M. Aziz, F. Atmani, A. Remmal, A. Ziyyat, J. Ethnopharmacol. **94**, 317 (2004)
26. N.S. Sandhu, S. Kaur, D. Chopra, Asian J. Pharm. Clin. Res. **3**, 146 (2010)
27. S. Soleimani, F.F. Azarbaizani, V. Nejati, Pak. J. Biol. Sci. **10**, 4236 (2007)
28. N. Radulović, G. Stojanović, R. Palić, Phytother. Res. **20**, 85 (2006)
29. M. Veit, C. Weidner, D. Strack, V. Wray, L. Witte, F.C. Czygan, Phytochemistry **31**, 3483 (1992)
30. A. Carnet, C. Petitjean-Freytet, D. Muller, J. Lamaison, Plants Med. Phytother. **25**, 32 (1991)
31. J.G. dos Santos Junior, F.H.M. do Monte, M.M. Blanco, VMdNB Lanziotti, F.D. Maia, L.K. de Almeida Leal, Pharmacol. Biochem. Behav. **81**, 593 (2005)
32. M. Veit, K. Bauer, H. Geiger, F.C. Czygan, Planta Med. **58**, 697 (1992)
33. B. Fabre, B. Geay, P. Beaufils, Plantes Med. Phytother. **26**, 190 (1993)
34. C. Beckert, C. Horn, J.P. Schnitzler, A. Lehning, W. Heller, M. Veit, Phytochemistry **44**, 275 (1997)
35. T. Řezanka, Phytochemistry **47**, 1539 (1998)
36. F. Adam, K. Kandasamy, S. Balakrishnan, J. Colloid Interface Sci. **304**, 137 (2006)
37. B.M. Cherian, L.A. Pothan, T. Nguyen-Chung, G. Mennig, M. Kottaisamy, S. Thomas, J. Agric. Food Chem. **56**, 5617 (2008)
38. X. Sun, F. Xu, R. Sun, P. Fowler, M. Baird, Carbohydr. Res. **340**, 97 (2005)
39. D. An, Y. Guo, Y. Zhu, Z. Wang, Chem. Eng. J. **162**, 509 (2010)
40. L. Sapei, N. Gierlinger, J. Hartmann, R. Nöske, P. Strauch, O. Paris, Anal. Bioanal. Chem. **389**, 1249 (2007)
41. P. Yuan, P.D. Southon, Z. Liu, M.E.R. Green, J.M. Hook, S.J. Antill, C.J. Kepert, J. Phys. Chem. C **112**, 15742 (2008)
42. M. Thommes, Chem. Ing. Tech. **82**, 1059 (2010)
43. N. Yalcin, V. Sevinc, Ceram. Int. **27**, 219 (2001)
44. M.G. Dekamin, M. Eslami, Green Chem. **16**, 4914 (2014)
45. M.A. Zolfigol, N. Bahrami-Nejad, F. Afsharnadery, S. Baghery, J. Mol. Liq. **221**, 851 (2016)
46. A. Rostami, B. Atashkar, H. Gholami, Catal. Commun. **37**, 69 (2013)
47. S. Rostamnia, A. Nuri, H. Xin, A. Pourjavadi, S.H. Hosseini, Tetrahedron Lett. **54**, 3344 (2013)
48. S. Balalaie, M. Bararjanian, M. Sheikh-Ahmadi, S. Hekmat, P. Salehi, Synth. Commun. **37**, 1097 (2007)
49. R.-Y. Guo, Z.-M. An, L.-P. Mo, R.-Z. Wang, H.-X. Liu, S.-X. Wang, Z.-H. Zhang, ACS Comb. Sci. **15**, 557 (2013)
50. M.A. Zolfigol, M. Safaiee, N. Bahrami-Nejad, New J. Chem. **40**, 5071 (2016)
51. M. Amirnejad, M.R. Naimi-Jamal, H. Tourani, H. Ghafuri, Monatsh. Chem. **144**, 1219 (2013)

52. S. Gao, C.H. Tsai, C. Tseng, C.-F. Yao, Tetrahedron **64**, 9143 (2008)
53. P. Sharma, M. Gupta, R. Kant, V.K. Gupta, RSC Adv. **6**, 32052 (2016)
54. B. Sadeghi, A. Hassanabadi, S. Bidaki, J. Chem. Res. **35**, 666 (2011)
55. H. Naeimi, M. Farahnak Zarabi, Appl. Organomet. Chem. **32**, e4225 (2018)
56. S. Nemouchi, R. Boulcina, B. Carboni, A. Debache, C. R. Chim. **15**, 394 (2012)
57. S. Banerjee, A. Horn, H. Khatri, G. Sereda, Tetrahedron Lett. **52**, 1878 (2011)
58. V. Safarifard, S. Beheshti, A. Morsali, CrystEngCommun **17**, 1680 (2015)
59. S. Pradhan, V. Sahu, B.G. Mishra, J. Mol. Catal. A Chem. **425**, 297 (2016)
60. A. Maleki, R. Ghalavand, R. Firouzi Haji, Appl. Organomet. Chem. **32**, e3916 (2018)
61. Y. Sarrafi, E. Mehrasbi, A. Vahid, M. Tajbakhsh, Chin. J. Catal. **33**, 1486 (2012)
62. K. Niknam, M. Khataminejad, F. Zeyaei, Tetrahedron Lett. **57**, 361 (2016)
63. A. Hasaninejad, M. Shekouhy, N. Golzar, A. Zare, M.M. Doroodmand, Appl. Catal. A Gen. **402**, 11 (2011)
64. M. Abdollahi-Alibeik, F. Nezampour, React. Kinet. Mech. Catal. **108**, 213 (2013)
65. R.S. Bhosale, C.V. Magar, K.S. Solanke, S.B. Mane, S.S. Choudhary, R.P. Pawar, Synth. Commun. **37**, 4353 (2007)
66. B. Maleki, S.S. Ashrafi, RSC Adv. **4**, 42873 (2014)
67. D. Azarifar, S.M. Khatami, M.A. Zolfigol, R. Nejat-Yami, J. Iran. Chem. Soc. **11**, 1223 (2014)
68. R. Heydari, R. Rahimi, M. Kangani, A. Yazdani-Elah-Abadi, M. Lashkari, Acta Chem. Iasi **25**, 163 (2017)
69. A.A. Mohammadi, M.R. Asghariganjeh, A. Hadadzahmatkesh, Arab. J. Chem. **10**, S2213 (2017)
70. P. Bhattacharyya, K. Pradhan, S. Paul, A.R. Das, Tetrahedron Lett. **53**, 4687 (2012)